NUMERICAL SIMULATION OF SUPERCRITICAL PRESSURE FLUIDS WITH VARIABLE TURBULENT PRANDTL NUMBER AND MODIFIED DAMPING FUNCTION (1/2)

Y. Y. Bae, E. S. Kim, M. H. Kim,
Korea Atomic Energy Research Institute,
Daedeokdaero 989-111, Yuseong, Daejeon, Republic of Korea
Email: yybae@kaeri.re.kr

ABSTRACT

In most numerical simulations of a fluid flow with constant properties or negligible variations, the value of Pr_t has been considered to be unity or close to it. However, numerical attempts with a constant Pr_t have never been successful in estimating the wall temperature in highly-buoyant supercritical fluids through vertical tubes. Several experimental data and numerical studies have indicated that Pr_t can be very smaller or larger than unity in a region of severe property variation. Recent research, both numerical and experimental, indicate that Pr_t is very likely a function of fluid-thermal variables, when the gradients of the physical properties of the fluid are significant. In this regard, a new concept of a variable turbulent Pr_t according to the property variation was developed. Another point to be considered is that the turbulent boundary layer (TBL) deforms so severely that the damping function included in the turbulence modeling is no longer a fixed function of the turbulence properties. When a velocity overshoot (or peak) appears in or near the TBL, a new TBL may develop between the point of the velocity peak and the wall. Accordingly, the damping function in the new TBL will be different from that for the TBL without a velocity peak. A new formulation for the damping function, actually the thickness of the viscous sublayer, A^+, was introduced to accommodate the TBL deformation. The new formulations for Pr_t and A^+ were tested in the numerical simulation, and the results agreed well with the experimental data.

KEYWORDS
Mixed convection, supercritical pressure, turbulent Prandtl number, viscous sublayer

1. INTRODUCTION

When the fluid temperature approaches the pseudo-critical point at a supercritical pressure, it experiences a severe property variation resulting in tremendous difficulties in numerical simulations. Earlier numerical simulations have shown, without exception, an over-prediction of the experimental data with strong buoyancy. The over-predictions might have been derived from an inapplicability of widely used turbulence models as well as the constant turbulent Prandtl number (Pr_t).

Owing to the difficulties in numerical simulations, most earlier works were experimental and usually tried to develop correlations. A number of correlations for the prediction of the heat transfer rate in fluids at supercritical pressures have been proposed by various researchers, but most of them are valid only in a forced convection regime, as shown in the review paper by Cheng and Schulenberg [1], and a monograph by Pioro and Duffey [2]. The correlations available in published papers predict the heat transfer rate with a reasonable accuracy in a forced convection regime. However, in a mixed convection regime, all of these correlations fail to produce accurate predictions. IAEA sponsored and led to collaborative work among the various universities and institutions all over the world, and published a TECDOC [3], which

summarizes the current state-of-art research information on a supercritical heat transfer.

A number of numerical works have been conducted to simulate the flow and thermal field of a fluid flowing at a supercritical pressure, and in doing so, the applicability of various turbulence models was examined. For both forced and mixed convection regimes, experimental and numerical investigations of the thermal and flow field at supercritical pressure was performed by Licht et al. [4]. They confirmed that for a simple case of deterioration, simulations using Fluent offered a qualitative insight into changes in fluid temperature and turbulent velocities responsible for the axial evolution of the wall temperature. Cho et al. [5] examined three turbulence models, i.e., RNG k-e, SST k-ω, and one type of low-Reynolds number model, against the experimental data obtained for a tube and annulus with an equivalent hydraulic diameter of 4.4 mm, and reported that the performance of the three models was partially successful. He et al. [6] thoroughly investigated low- Reynolds number turbulence models and concluded that both the low Reynolds number k-ε models and the V2F models were able to capture the general trends of the interesting wall temperature behavior observed with an upward flow in some experiments with a fluid at a pressure just above the critical value, while the detailed variation of the wall temperature predicted by using each model was rather different from that in the experiments. They also found that the effect on the heat transfer was almost entirely due to the shear production effect caused by the distortion of the mean low as a result of the strong influence of buoyancy. Using a modified version of a low-Reynolds turbulence model, Zhang et al. [7] successfully reproduced the data from a DNS calculation and an experiment by employing an algebraic flux model in calculating the turbulence production by buoyancy. However, its application to the other conditions is still to be proven. Zhang et al. [8] compared the experimental data of a heat transfer in supercritical fluids in a circular tube with the calculation results obtained by employing six different turbulence models and found that the Reynolds stress model (RSM) gave the best agreement with the experimental data, especially with the data including deteriorated heat transfer. The result of the RSM was not much different from that of RNG k-e, and its applicability should be considered in parallel with the fact that it requires solving additional equations. As discussed above, the numerical simulations for the highly buoyant flow failed to reproduce the particularly thermal field. This situation forced us to revisit the turbulence modeling and Pr_t and to carefully review the turbulent boundary layer theory, which are the basis of them.

In most numerical simulations of a fluid flow with constant properties or negligible variations, the value of Pr_t has been considered to be unity or close to it; and the results agreed with the experimental data very well. However, the numerical works with a constant Pr_t have failed or been only partially successful in estimating the wall temperature in highly-buoyant supercritical fluids through vertical tubes. Several experimental data and numerical studies have indicated that the Pr_t can be much smaller or larger than unity in a region of severe property variation. Recent research [9,10], both numerical and experimental, had indicated that the Pr_t was very likely a function not only of fluid but also of physical properties , when the gradients of physical properties of fluid are significant. In this regards, a new concept of a variable turbulent Pr_t according to property variation was developed.

As another point to be considered in the numerical simulation of fluids with strong property variations, the TBL deforms so severely that a fixed damping function is no longer applicable, and should be adjusted according to the degree of deformation. When a velocity overshoot (or peak) appears in or near the TBL, a new TBL may develop between the point of the velocity peak and the wall. Accordingly, the damping function in the new TBL will be different from the one for the TBL without a velocity peak. A simple function was introduced to accommodate the alteration of the damping function (or viscous sublayer thickness). In a conventional damping function, 1- e^{-y+/A^+} A^+ represents the thickness of the viscous sublayer. When the flow field undergoes a strong deformation, the shear stress will also alter, and is manifested in an altered value of A^+.

In this paper, an attempt will be made to formulate a variable Pr_t and find a functional relation between A^+

and shear stress in the TBL.

2. METHOD OF ANLYSIS

2.1. Turbulent Prandtl Number

Reynolds [11] reviewed more than thirty ways for predicting Pr_t and the Schmidt number (Sc_t). Kays [12] examined the then-available experimental data on Pr_t for the two-dimensional TBL. Pr_t has been treated as a constant of around 0.9 or unity in most earlier numerical works. However, there are other cases where Pr_t is far from unity. Pr_t becomes approximately 0.7 for an axi-symmetric case of a heated jet, while planar jet data indicate a value of 0.5; in a thermally developing wall bounded TBL, Pr_t is around unity only in the core boundary layer, and it decreases to a value of less than 0.5 [13]. In a TBL, Pr_t decreases from around 1.5 in the sub-layer to 0.7 at the outer edge of the boundary layer [14]. According to the experiment data provided by Dai et al. [9], the value of Pr_t reaches as small as 0.05. The above evidence strongly implies that Pr_t can hardly be unity or a constant very close to it at least in the case of heating or cooling of fluid experiencing a substantial property variation. Pr_t is purely a product of the Reynolds analogy, which claims that the mechanism of turbulent heat transfer would be very similar to that of the turbulent momentum transfer.

An assessment of Pr_t for case (C) published in [15] was made, and the result is shown in Figure 1. Evidently, Pr_t has values much less than unity inside the turbulent boundary layer, especially in the buffer and viscous sublayer. The peaks are due to the strong gradient of the velocity and temperature, which is an inevitable irregularity originated from the application of the gradient diffusion hypothesis in the turbulent momentum and energy diffusion. It should be noted that the values of Pr_t continuously decrease toward the wall, contrary to the well-known experimental evidences, where, without exception, Pr_t increased toward the wall.
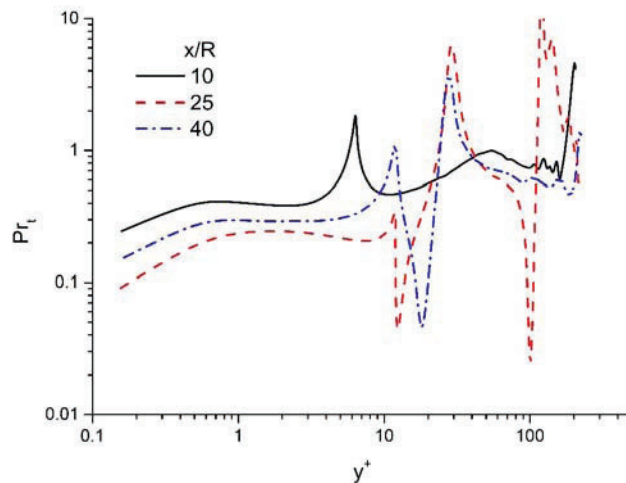

Figure 1. Variation of Pr_t with y^+ at three axial locations. G = 166.62 kg/m2s, q = 30.87 kW/m2, P = 8.0 MPa, d = 2 mm. Deduced from [15].

First, let us examine the steps taken to derive the Reynolds analogy for the turbulent heat transfer (the discussion of Kay et al. [16] was largely followed.). Imagine an element of fluid of mass δm that moves

in the y direction at distance ℓ (which is a "mixing length"). Let us assume that the effective velocity of fluid in the y ($= R\text{-}r$) direction is $C\sqrt{v'^2}$. According to the momentum theorem, the shear force is equal to the rate of momentum transfer. Then, the effective shear stress is

$$\tau_t = \frac{F}{A} = C\sqrt{\overline{v'^2}}\,\delta\!\left(\overline{\rho u}\right) = C\sqrt{\overline{v'^2}}\left(\overline{\rho}\,\delta\overline{u} + \overline{u}\,\delta\overline{\rho} + \delta\overline{u}\,\delta\overline{\rho}\right) \tag{1}$$

The over-bar implies that the quantities are Reynolds-averaged.
Similarly, the effective heat flux is

$$\dot{q}''_t = C\sqrt{\overline{v'^2}}\,\delta\!\left(\overline{\rho c_p T}\right) = C\sqrt{\overline{v'^2}}\left(\overline{\rho c_p}\,\delta\overline{T} + \overline{\rho T}\,\delta\overline{c}_p + c_p\overline{T}\,\delta\overline{\rho} + \overline{\rho}\,\overline{c}_p\,\delta\overline{T} + c_p\,\delta\overline{\rho}\,\delta\overline{T} + \overline{T}\,\delta\overline{\rho}\,\delta\overline{c}_p\right) \tag{2}$$

If the functional relations of incremental variation of the variables, $\delta\overline{u}$, $\delta\overline{\rho}$, $\delta\overline{c}_p$ and $\delta\overline{T}$ with respect to each other across distance ℓ are known, the exact value of Pr_t can be calculated. In a conventional approach, the property variation was generally neglected under the assumption of constant properties or a negligible variation of them. However, for a fluid at supercritical pressure, the two terms in the far right-hand side of Eq. (1) and the five terms in the far right-hand side of Eq. (2) are no longer negligible, and can possibly be greater than the remaining terms. The second-order terms should not be neglected, if an extremely accurate prediction is required, since they amount to greater than 1% at some locations. When the mixing distance is sufficiently small, the increments $\delta\overline{u}$, $\delta\overline{T}$, $\delta\overline{\rho}$ and $\delta\overline{c}_p$ can be safely expressed as the mixing length times their gradient.

From the definition of momentum and thermal diffusivity,

$$\frac{\tau_t}{\rho} = \nu_t\frac{\partial\overline{u}}{\partial y}, \qquad \frac{\dot{q}''_t}{\overline{\rho}c_p} = \alpha_t\frac{\partial\overline{T}}{\partial y} \tag{3}$$

Eqs. (1) and (2) are provided for $\mathrm{Pr}_{t,vp} = \nu_t/\alpha_t$.

$$\mathrm{Pr}_{t,vp} = \cfrac{1 + \cfrac{\overline{u}}{\overline{\rho}}\left|\left(\cfrac{\partial\overline{\rho}}{\partial y}\right)\middle/\left(\cfrac{\partial\overline{u}}{\partial y}\right)\right| + \cfrac{\ell}{\overline{\rho}}\left|\cfrac{\partial\overline{\rho}}{\partial y}\right|}{1 + \cfrac{\overline{T}}{\overline{\rho}}\left|\left(\cfrac{\partial\overline{\rho}}{\partial y}\right)\middle/\left(\cfrac{\partial\tilde{T}}{\partial y}\right)\right| + \cfrac{\overline{T}}{\overline{c}_p}\left|\left(\cfrac{\partial\overline{c}_p}{\partial y}\right)\middle/\left(\cfrac{\partial\overline{T}}{\partial y}\right)\right| + \cfrac{\ell}{\overline{c}_p}\left|\cfrac{\partial\overline{c}_p}{\partial y}\right| + \cfrac{\ell}{\overline{\rho}}\left|\cfrac{\partial\overline{\rho}}{\partial y}\right| + \cfrac{\ell\overline{T}}{\overline{\rho c}_p}\left|\cfrac{\partial\overline{\rho}}{\partial y}\cfrac{\partial\overline{c}_p}{\partial y}\left(\cfrac{\partial\overline{T}}{\partial y}\right)^{-1}\right|} \tag{4}$$

In a practical sense, the terms including the mixing length in Eq. (4) can be neglected, since they are negligibly smaller than the other terms. The subscript "vp" was added to indicate the turbulent Prandtl number is based on the physical properties.

The value of $\mathrm{Pr}_{t,o}$ approaches unity or even a large number when the value of y^+ is smaller than 10. In a viscosity-dominated region, the turbulent heat flux will also be suppressed as much as the turbulent momentum transfer. Therefore, it was assumed that Pr_t dies down toward the wall, following the same manner of the turbulent momentum transfer. The above argument allows us to introduce the following function, which is exactly the same as the damping function originally proposed by Van Driest, as the first factor to be added to the variable Pr_t.

$$f_1 = 1 - \exp\left(-\frac{y^+}{A^+}\right) \quad (5)$$

Considering that all gradients in the flow variables and fluid properties will be reduced to zero around the tube center line, Pr_t is expected to approach a standard value, say, σ_t (= 0.9), in this direction as it does toward the wall. Therefore, the following function is introduced to take this assumption into account.

$$f_2 = 0.5\left[1 + \tanh\left(\frac{B - y^+}{10}\right)\right] \quad (6)$$

The function f_2 is completely arbitrarily, and any other function, which guarantees a smooth transition from the TBL to centerline, should be acceptable.
The constant 10 is an arbitrary value given to make sure that the function f_2 varies smoothly around $y^+ = B$. The value of B should be carefully determined to make sure that beyond the point of $y^+ = B$, the flow is in the wake region. Pr_t derived here is valid only in the TBL and not in the wake region, where the mixing length theory is no longer valid. In a TBL, the log-law and wake region are separate from each other at around $y^+ = B$, and the momentum diffusivity asymptotically reaches a constant value as it enters the wake region, as can be found in the textbook dealing with TBL [13, 16]. The experimental data provided by Quarmby and Quirk [17] and Dai el al. [9] show that it may be natural to assume that Pr_t asymptotically converges to 0.9 as y approaches R, say the tube centerline or axis. In the case of TBL on a flat plate, the boundary condition for ε at the TBL outer edge is given as a free stream value. This cannot be the case for a TBL in a pipe, since ε is calculated as a part of the solution rather than being defined or given. As can be seen in references [18,19], ν_t/ν asymptotically approaches a constant value, where theoretically every property or variable should have nearly zero gradients. It is strongly indicated that Pr_t has a constant value being close to a conventional value of 0.9; this is consistent with the fact that Pr_t asymptotically approaches a constant in TBL on a flat plate with a zero pressure gradient [20].

Finally, with the incorporation of the functions introduced above, the variable Pr_t takes the following form.

$$Pr_t = \sigma_t - f_1\, f_2\left(\sigma_t - Pr_{t,vp}\right) \quad (7)$$

Although Eq. (7) was derived through a non-rigorous manner and are considered arbitrary, it proved to produce results agreeing pretty well with the experimental data when applied to the computational works. The mode detailed discussion of the Pr_t can be found in the authors' companion paper [21].

2.2. Behavior of Viscous Sublayer under Strong Property Gradient

When a fluid moves at a supercritical pressure, its properties substantially vary across the pseudo-critical temperature. In particular, the decrease in density has the strongest influence on the fluid-thermal behavior through buoyancy force.

After performing extensive numerical calculations, it was found that the velocity peak (a local maximum velocity or overshoot where $\partial\bar{u}/\partial y = 0$) starts to appear in the far outer boundary layer and moves into the boundary layer, and after reaching a certain point, fades back away from the wall. Figure 2 shows the variation of the location where the axial velocity reaches the maximum. The peak moves into the

boundary layer very quickly and it slowly fades away. Under this circumstance, it is very unlikely that the viscous sublayer remains the same as in many previous numerical works. The existence of the velocity peak alters the TBL, and it is manifested in the change of the viscous sublayer. The eddy viscosity model based on the Van Driest mixing length model based on the flat-plate flow with no mass transfer cannot be used in the case with a strong buoyancy, since the TBL with a strong buoyancy as well as non-uniform properties is quite different from that for a flat-plate flow with constant properties. As discussed in the monograph by Cebeci [22], the viscous sublayer, which appears in the damping function as A or A^+, changes according to the pressure gradient and mass transfer (or wall injection). The effect of the pressure gradient and mass transfer appears in the change of the shear stress at the intersection of the linear law of the wall and the log-law of the wall. After an examination of the equation for τ_s/τ_w it was concluded that the equations appearing in [22] cannot be directly applied. The influence of the pressure gradient is considered different from that of the buoyancy. From the discussions given by Cebeci, it was found that the deformation of TBL leads to a change in the shear stress in the buffer region, and it is finally manifested in the ratio of shear stress between the buffer layer and wall. The shear stress ratio is related with the viscous sublayer thickness.
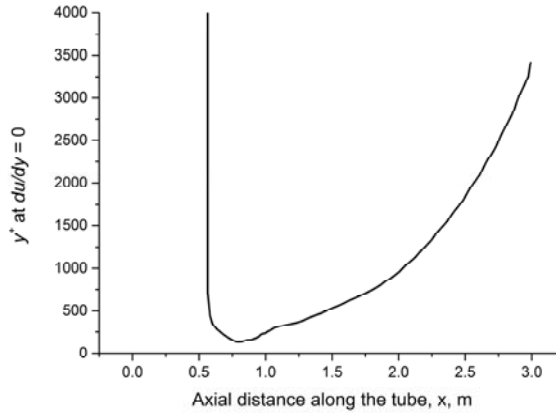
Figure 2. Variation of the location where the axial velocity reaches maximum or $du/dy = 0$.
Water, $P = 23$ MPa, $G = 600$ kg/m²s, $q = 600$ kW/m²

Jackson [3,23] developed a semi-empirical model of a fully developed mixed convection in a vertical tube to account for the strong non-uniformity of fluid properties, such as the buoyancy and acceleration, as follows.

$$\frac{\tau_{\delta_t}}{\tau_w} = 1 - \left(C_A Ac_b + C_B Bo_b F_{VP3} F_{VP4}\right) F_{VP1} \left(\frac{\tau_{\delta_t}}{\tau_w}\right)^{-1/2} \tag{8}$$

where τ_{δ_T} is the shear stress at the buffer layer, and C_A and C_B are constant coefficients.

$$Ac_b = Q_b / \mathrm{Re}^{1.625} \mathrm{Pr}_b \ , \ Bo_b = \mathrm{Gr}_b / \mathrm{Re}_b^{2.625} \mathrm{Pr}_b^{0.4} \ , \ F_{VP3} = \left(\frac{\overline{\mathrm{Pr}}}{\mathrm{Pr}_b}\right)^{-0.4} \ , \ F_{VP4} = \left(\frac{\rho_b - \overline{\rho}}{\rho_b - \rho_w}\right),$$

and $F_{VP1} = \left(\overline{\mu}/\mu_b\right)\left(\overline{\rho}/\rho_b\right)^{-1/2}$. Ac_b and Bo_b are the acceleration and buoyancy parameters, respectively. F_{VP1}, F_{VP1}, and F_{VP3} are parameters reflecting the property variation across the TBL. Q_b is a dimensionless

thermal expansion group, $\beta_b q_w D / k_b$. Subscripts b and w imply the bulk and wall conditions, respectively. Other dimensionless groups have conventional meanings. For the cases dealt with in this paper, the values of Ac_b were negligibly smaller than that of Bo_b. In other words, the effect of acceleration was negligibly smaller than the buoyancy. The acceleration coefficient C_A has an estimated value of 10,000 for an assumed value of δ^+ of 30. The buoyancy coefficient C_B is 4,600 based also on $\delta^+ = 30$. Please note that the minus sign in Eq. (8) corresponds to the upward flow, and it should be replaced with a plus sign for a downward flow.

We assumed that the relation between the viscous sublayer thickness and the shear stress follows the same relation as discussed by Cebeci [22], that is, the viscous sublayer thickness, A^+, is a function of the square root of τ_s / τ_w. It should be noted that τ_s is the same as τ_{δ_T}. The solution of Eq. (8) can be expressed in the following equations after fitting.

$$
\begin{aligned}
&(\tau_s / \tau_w)^{1/2} = (1 - 2.35Z)^{0.2} \quad \text{for} \quad Z < 0.383 \\
&(\tau_s / \tau_w)^{1/2} = 0.26 + 0.48Z - 0.07Z^2 + 0.006Z^3 \\
&\qquad\qquad - 2.57 \times 10^{-4} Z^4 + 4.28 \times 10^{-6} Z^5 \quad \text{for} \quad Z > 0.383
\end{aligned}
\tag{9a,b}
$$

where $Z = Z_{Ac} + Z_{Bo} = C_A Ac_b F_{VP1} + C_B Bo_b F_{VP1} F_{VP3} F_{VP4}$, and it will be referred to as a dimensionless boundary layer deformation (BLD) parameter. Z_{Ac} and Z_{Bo} are the dimensionless BLD parameters attributed to the acceleration and buoyancy. The exact solution of Eq. (8) is 0.5777 for $Z = 0.3849$, which is obviously different from the value obtained from Eq. (**9**a), which are the curve fitted from the solution of Eq. (8).

It would not be unreasonable to assume that the value of A^+ is a function of τ_s / τ_w as shown in [22], although in a different functional form. When the velocity peak appears sufficiently far from the wall such that the effect of the appearance of the velocity peak is barely felt by the viscous sublayer. Considering the asymptotic behavior of τ_s / τ_w for small values of Z, it can be safely assumed that A^+ also behaves in a similar manner to that of τ_s / τ_w. Thus, it is assumed that A^+ and τ_s / τ_w have the following relation.

$$
A^+ / A_o^+ = f_1 = (\tau_s / \tau_w)^{1/2}
\tag{10}
$$

where A_o^+ was set as 70 as proposed by Myong and Kasagi [24] and the function f_1 is defined in Eq. (**9**a). Eq. (**10**) is different from that in [22], where A^+ was inversely proportional to $(\tau_s / \tau_w)^{1/2}$. Eq. (**10**) is physically more plausible since the occurrence of the velocity peak narrows the TBL and forces it to restructure between the wall and the location of the velocity peak. If this is so, the viscous sublayer will shrink proportionally to the shrinking of the TBL.

As the location of the velocity peak penetrates further into the TBL, the situation becomes different from the argument given above. Once the location of the velocity peak enters the region of the log-law of the wall, it severely disturbs the viscous sublayer, and Eq. (10) will become no longer valid. In this case, the low density fluid is concentrated near the wall. The low-density fluid region can be treated as fluid injection from a porous wall. The existence of the velocity peak is due to the extra volumetric flow

originated from the density decrease. The extra volumetric flow can be considered as a mass injection through the wall in a constant-property flow. The apparent dimensionless injection velocity v_w^+ can be expressed as

$$v_w^+ = \frac{\bar{u}}{u_\tau} \frac{\rho_{\delta_T} - \bar{\rho}}{\rho_{\delta_T}}, \tag{11}$$

ρ_{δ_T} is the density at the edge of the viscous sublayer. With the introduction of the idea of apparent mass injection, the expression proposed by Cebeci [22] may serve our purpose. Without a pressure gradient, the relation between A^+ and v_w^+ proposed in [22] is

$$A^+/A_o^+ = f_2 = \exp(-5.9v_w^+). \tag{12}$$

The examination of v_w^+ showed that its order of magnitude is very similar to that of Z. Accordingly, it can be assumed that Eq. (12) determines the value of A^+ when v_w^+ is replaced with Z. Eqs. (10) and (12) determine the value of A^+ in two extreme cases. Obviously, they do not smoothly connect to each other. In this regard, arbitrary hybrid functions are introduced. From the numerical experiment, it was found that the function connecting Eqs. (10) and (12) showed a hysteresis. The variation of A^+ from Eqs. (10) through (12) does not follow the path in Eqs. (12) and (10). In this regard, the following two hybrid functions were introduced.

$$\begin{aligned} g_1 &= 0.5\{1 + \tanh[(Z - 0.35)/0.01]\} \\ g_2 &= 0.5\{1 + \tanh[(Z - 0.2)/0.01]\} \end{aligned} \tag{13a,b}$$

Eqs. (13a,b) are totally arbitrary and should be verified experimentally. However, it would serve the present purpose of the numerical experiment. Figure 3 shows the variation of A^+/A_o^+ with Z. As Z increases, A^+/A_o^+ decreases following function f_1 [Eq. (9a)] and at a certain value of Z, it jumps onto function f_2 [Eq. (12)] following the hybrid function g_1. As the flow passes its maximum buoyancy or acceleration, Z decreases, and after following Eq. (12) to a certain value of Z and returns to Eq. (10) through the hybrid function g_2. The relations among the functions f_1, f_2, g_1 and g_2 are graphically shown in Figure 3.

2.3. Numerical Method

In the present study, a vertically upward flowing fluid in a uniformly heated tube was considered. The flow was assumed to be steady and 2-D axi-symmetric. The vertical upward direction was aligned in the positive x direction, and the radial coordinate was r. In the circumferential direction, the velocity components as well as the gradient of all flow and thermal properties were assumed to be zero. That is, there is no swirl. The governing equations employed in the present study were a continuity equation, ensemble averaged Navier-Stokes equation, energy equation, and two-equation turbulence model. The governing equations for a velocity field in a cylindrical coordinate with a two-equation k-e turbulence

model can be found in [6], and will not be repeated here. The low-Reynolds number turbulence model proposed by Myong and Kasagi [24] was used in this paper.
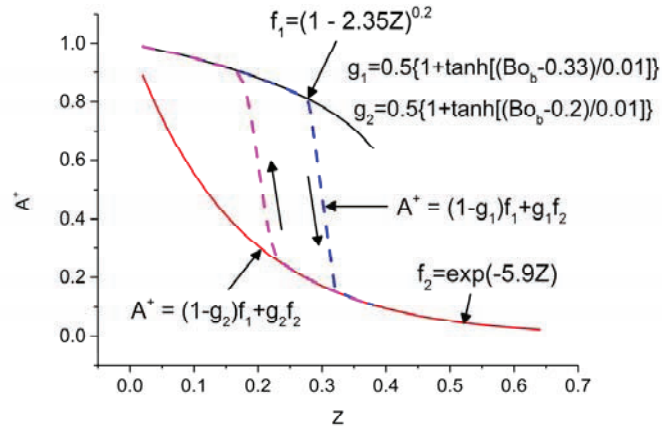

Figure 3. Variation of $A+$ with Z.

The present numerical study was conducted using an in-house code, a version modified from the one provided by Ferziger and Peric [25]. Basically, the SIMPLE algorithm with a single pressure correction step was applied. All variables were assigned to the collocated grids. Diffusive fluxes were discretized by busing the power law scheme, while for convective fluxes, a linear interpolation was allowed to be blended with an upwind approximation. The resulting matrix of the variables was iteratively solved using Stone's SIP (strongly implicit procedure) method. The computational object was a vertical upward flow of water and carbon dioxide in uniformly heated circular tubes with several different diameters.

The fully developed turbulent flow was used as an inlet velocity profile. An unheated section was provided in front of the heated section. The length was different among the cases. It did not give any significant effect on the calculation. The calculation domain was discretized into rectangular grids. The grid was refined into the wall in the radial direction. After trying several values of y_P^+ (the value of y^+ at the first node from the wall), $y_P^+ < 0.5$ was found to be optimum with the result of reasonably accurate converged solutions. Further refinement results in an unnecessarily long computing time with no improvement of the calculation accuracy.

Although there is no unique definition of the normalized wall distance y^+, most of the computational works performed thus far, regardless of compressible or incompressible cases, employed the definition $y^+ = u_\tau y / \nu_w$, where $u_\tau = (\tau_w / \rho_w)^{1/2}$ using wall properties. Instead, in this work, an altered definition based on the local properties such as $y^+ = (\tau_w / \rho)^{1/2} y / \nu$, which is called the semi-local scaling, was used. The only reason for the choice was that the computational results obtained in this work with the latter definition agreed with the experimental results better than those with the former definition. When only a narrow region near the wall is heated to high temperature, the use of $u_\tau = (\tau_w / \rho_w)^{1/2}$ will result in an unrealistically high value of y^+, making the damping function approach unity more rapidly as y^+ increases. When the physical properties vary considerably, the definitions of u_τ and y^+ greatly influence the numerical results through the damping function and coefficients involving y^+ as an independent variable. An exact assessment of the effect of the definitions of u_τ and y^+ is not available at the moment and is left for further research. Huang et al. [26] also indicated that semi-local scaling was the best in the

interpretation of their DNS calculation results of compressible turbulent channel flows. Foysi et al. [27] reported that the use of semi-local scaling improved the similarity in the turbulence, although a global similarity was not achieved.

From the experiment of the turbulent boundary layer it is known that the viscous sublayer, especially the linear law of the wall region, remains unchanged regardless of the disturbance. During the calculation, the value of A^+ was not allowed to be smaller than 10, which is the typical thickness of a viscous sublayer.

3. RESULTS AND DISCUSSIONS

Figure 4 shows the distribution of wall temperatures for the case of water flowing under the conditions of $G = 600$ kg/m^{2}s, $q = 600$ kW/m^2, and $P = 23$ MPa. When Pr_t and A^+ were set as constants 0.9 and 70, respectively, the maximum wall temperature reached 1309 K. The high temperature remained far downstream and the situation was hopeless owing to the fact that any turbulence modeling failed to reproduce the experimental data with strong buoyancy. This was confirmed here once again. With the introduction of the variable Pr_t, only the maximum wall temperature substantially reduced to 879 K, but was still much higher than the experimental data although the improvement was outstanding. With the application of both variables Pr_t and A^+ as a function of the parameters for buoyancy and acceleration, the maximum wall temperature reduced to 775 K, which was greater than the experimental data by only 30 K. The point of the maximum temperature appeared a little earlier than the experimental data, but the overall performance was excellent.

Figure 5 shows the variation of the dimensionless wall distance, y_o^+ (y^+ at $\partial u/\partial y = 0$), the viscous sublayer thickness, A^+, and the dimensionless boundary layer deformation parameter, Z, for the same case shown in Figure 4. Before the appearance of the velocity peak, the TBL was influenced by the buoyancy, and acceleration A^+ started decreasing. It should be noted that the minimum of A^+ did not coincide with the minimum of y_o^+. Because Z is less than 0.08, the value of A^+ was determined only by Eq. (10). Once the velocity appeared, the value of Z started decreasing. This is because of the decrease in Gr_b and the increase in Re due to the expansion of the low density region into the tube centerline. Again, the velocity peak disappeared very slowly. The good agreement of the numerical estimation with the experimental data indicates that the idea of variables Pr_t and A^+ is plausible. The spikes appearing at the front end of the heating are numerical oscillations originating from the severe property variation near the pseudo-critical temperature, and it was not possible to remove them completely using a grid refinement. The amplitude and frequency of the oscillation depended on the boundary conditions.

Figure 6 shows the distribution of the wall temperatures for the case of water flowing under the conditions of $G = 380$ kg/m^{2}s, $q = 417$ kW/m^2, and $P = 24.5$ MPa. As in the previous case, the numerical simulation highly over-predicted the experimental data. The effect of the variable Pr_t was surprisingly limited to the upstream of the maximum wall temperature. In the downstream of the maximum wall temperature, no improvement was seen. However, the overall numerical performance was still very poor. With the introduction of both variables Pr_t and A^+, the numerical performance was greatly improved, as shown in Figure 4. In the present calculation, the wall temperature peak shifted downstream. The overall numerical performance was very good except for the shift of the temperature peak.

Figure 7 shows the variation of y_o^+, A^+, and Z for the same case shown in Figure 6. Contrary to the previous case, the value of Z reached up to 0.33, which is very close to the maximum value of the validity of Eq. (9a), and did not fall down below 0.24. Obviously, the value of A^+ was determined by Eq. (9a) and Eq. (10) with the hybrid function, Eq. (13a), or possibly Eq. (13b). The velocity peak penetrated well into

the TBL and even reached the buffer layer. Under this circumstance, the viscous sublayer must be greatly influenced by the existence of the velocity peak. This is the reason for the failure of the well-known turbulence modelings, which are mostly based on the turbulence properties in a flat-plate flow. The introduction of both the variable Pr_t and A^+ greatly improved the numerical results. The calculated wall temperature agreed very well with the experimental data except for the shift of the temperature peak.
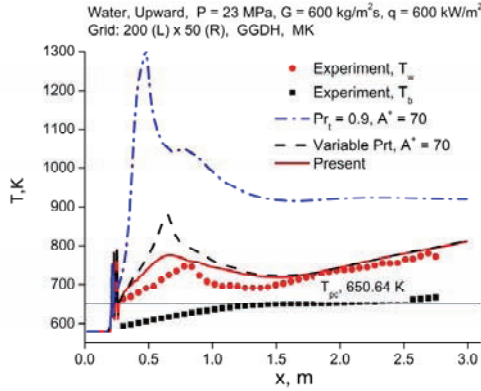
Figure 4. Distribution of the wall temperature along the tube. Experimental data after Zhao et al. [28].
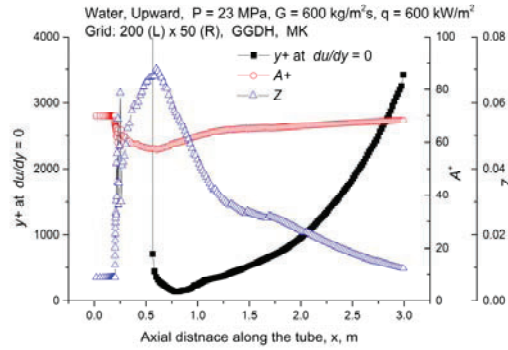
Figure 5 Distribution of y_o^+, A^+ and Z along the tube.

Distribution of y_o^+, A^+ and Z along the tube.
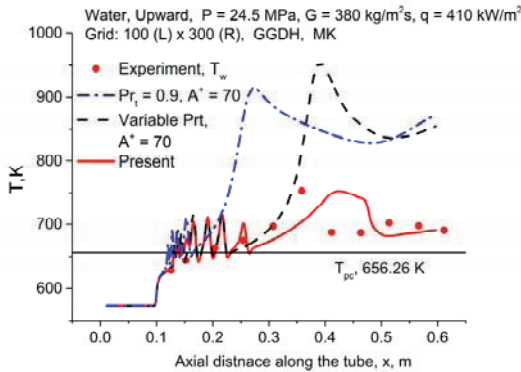
Figure 6. Distribution of the wall temperature along the tube. Experimental data after Alekseev et al. [29]
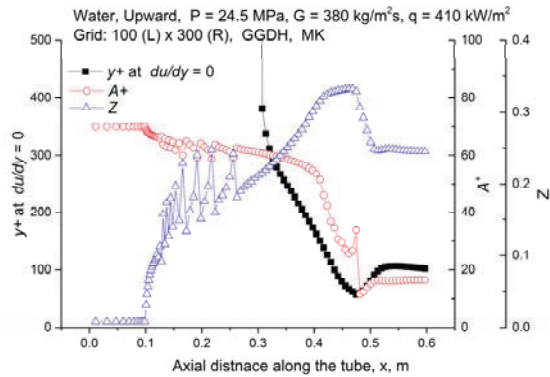

Figure 7. Distribution of y_o^+, A^+, and Z along the tube.

We would now like to compare the numerical results with the DNS data generated by Bae et al. [15]. Among the cases presented in [15], case C of mixed convection was chosen. Compared to the two previous cases for water, the effect of the variable Pr_t was negligibly small, as can be seen in Figure 8. With the introduction of variable A^+, the numerical results showed a good agreement with the experimental data. The difference of the maximum wall temperature between the calculation and experiment was less than 1 K. Again, the axial location of the maximum wall temperature appeared slightly downstream of that of the experimental data. The overall numerical performance seems reasonably satisfactory.

For the present case, the value of y_o^+ quickly penetrated deep into the log-law of the wall region, as shown in Figure 9. The minimum value of y_o^+ was 32.9. Consequently, the dimensionless parameter, Z, approached the maximum value of 0.53, which is much larger than the limiting value for Eq. (**9**a), 0.383, showing values larger than 0.3 over most of the heated section. As a result of the deep penetration of the velocity peak into the buffer region, the values of A^+ remain less than 20, resulting in a reduction of the wall temperature. The increase in Z generally reduces the Nusselt number, which is based on the bulk properties. However, the increase in Z simultaneously reduces the wall temperature by deforming the TBL, in other words, narrowing the viscous sublayer. At a certain value of Z, the wall temperature reducing effect of Z overwhelms the Nusselt number reduction (wall temperature increasing) effect, and the wall temperature actually starts decreasing after showing an increasing tendency.
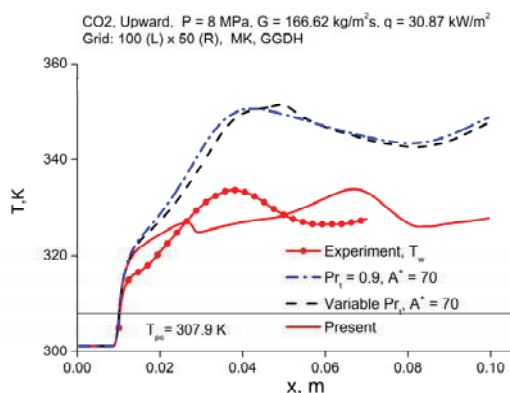

Figure 8. Distribution of the wall temperature along the tube. Experimental data after Bae et al. [15]
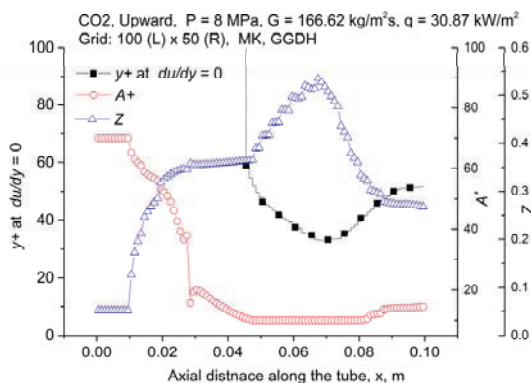
Figure 9. Distribution of y_o^+, A^+ and Z along the tube

Figure 10 shows the variation of the acceleration and buoyancy parameter, Z_{ac} and Z_{Bo}. For the case of water flowing upward under the conditions of $G = 600$ kg/m²s, $q = 600$ kW/m², $P = 23$ MPa (Figure 10a), Z_{Bo} dominated the Z_{ac} in the front part of the heating zone and then dropped to a value smaller than Z_{ac}. Judging from Figure 10a, it is advisable not to neglect the influence of the acceleration in the analysis of a flow with a strong buoyancy. The spike at the entrance region of the heated zone is associated with the numerical oscillation. In the case of CO_2 flowing upward under the conditions of $G = 166.62$ kg/m²s, $q = 30.87$ kW/m², and $P = 8$ MPa (Figure 10b), Z_{Bo} dominated Z_{ac} all over the heated zone. The overall dominance of Z_{Bo} is because the bulk temperature did not reach the pseudo-critical temperature at the exit of the heated zone. It is expected to drop down to a smaller value than Z_{ac} if the heated zone is sufficiently long. Clearly, the influence of the acceleration is not negligible in this case either.

4. CONCLUSIONS

An attempt was made to numerically simulate the highly buoyant flow with the introduction of variable Pr_t, and variable viscous sublayer thickness, A^+, appeared in the damping function included in the well-known turbulence modelings.

Pr_t was developed by extending the Reynolds analogy to include the effect of the property variation. A^+ was assumed to vary with the dimensionless buoyancy and acceleration parameters, Z_{Ac} and Z_{Bo}. The dependence of A^+ to Z_{Ac} and Z_{Bo} was assumed to be different between two zones divided by the value of

Z. For a smaller Z, A^+ was assumed to decrease in proportion to τ_s/τ_w, and for a larger Z, according to the exponential function of the dimensionless apparent wall injection, v_w^+.

(a)   (b)
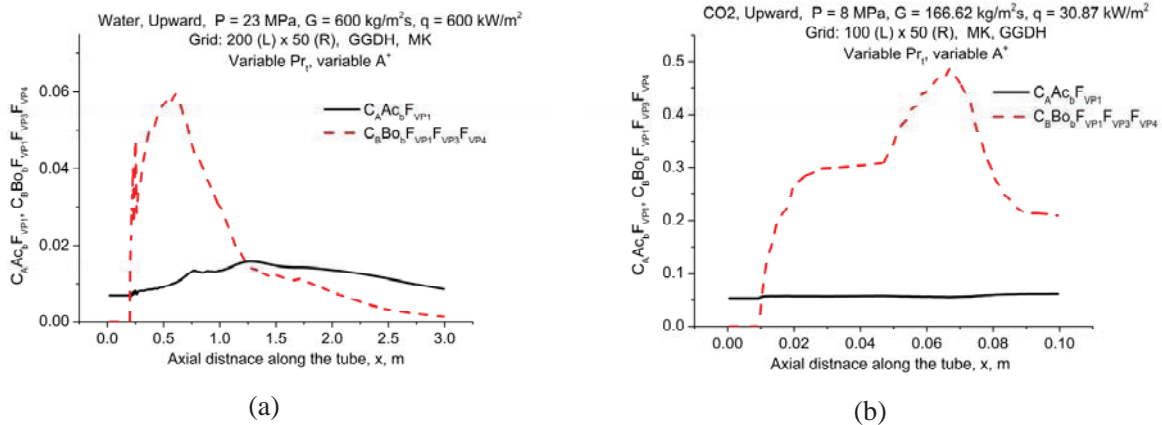
Figure 10. Variation of the ratio of acceleration parameter against buoyancy parameter.

The numerical simulations with the inclusion of variables Pr_t and A^+ resulted in an excellent agreement with the experimental and DNS data for water and CO_2. From the examination of Z_{Ac} and Z_{Bo} it was concluded that the influence of the acceleration should not be neglected.

Although a further refinement of the functions developed in this paper for the dependence of Pr_t and A^+ on the dimensionless boundary layer deformation parameter, Z, is necessary, it was clearly identified that the introduction of variables Pr_t and A^+ will lead to a better reproduction of the highly buoyant experimental data.

ACKNOWLEDGMENTS

REFERENCES

1. X. Cheng, T. Schulenberg, "Heat Transfer at Supercritical Pressures—Literature Review and Application to an HPLWR," Wissenschaftliche Berichte (Tech. Report) FZKA 6609, Forschungszentrum Karlsruhe, Mai, (2001).
2. I.L. Pioro, R.B. Duffey, *Heat Transfer and Hydraulic Resistance at Supercritical Pressures in Power-Engineering Applications,* ASME Press, New York (2007).
3. International Atomic Energy Agency, *Heat Transfer Behaviour and Thermalhydraulics Code Testing for Supercritical Water Cooled Reactors (SCWRs)*, Chapter 3 and 6, IAEA, Vienna (2014).
4. J. Licht, M. Anderson, M. Corradini, "Heat Transfer and Fluid Flow Characteristics in Supercritical Pressure Water," *J. of Heat Transfer*, **131**, 072502-1, July (2009).
5. B.H. Cho, Y.I. Kim, Y.Y. Bae, "Prediction of a heat transfer to CO2 flowing in an upward path at a supercritical pressure." *Nucl. Eng. Tech.*, **41**(7), pp. 907- 920 (2009).
6. S. He, W.S. Kim, J.D. Jackson, "A computational study of convective heat transfer to carbon dioxide at a pressure just above the critical value," *Applied Thermal Engineering*, **28**, pp. 1662–1675 (2008).

7. H, Zhang, Z.R. Xie, Y.H. Yang, "Numerical Study on Supercritical Fluids Flow and Heat Transfer under Buoyancy," *The 8th International Topical Meeting on Nuclear Thermal-Hydraulics, Operation and Safety (NUTHOS-8)* paper No.: N8P0187, Shanghai, China, October 10-14, (2010).

8. Y. Zhang, C. Zhang, J. Jiang, "Numerical Simulation of Heat Transfer of Supercritical Fluids in Circular Tubes Using Different turbulence Models," *J. of Nucl. Sci. and Tech.*, **48**(3), pp. 366–373 (2011).

9. Z. Dai, L-K. Tseng, G.M. Faeth, "Velocity/mixture fraction statistics of round self-preserving, buoyant turbulent flumes," HTD-Vol., **304**, (*95 National Heat Transfer Conference*-Volume 2), ASME (1995).

10. S.Kang, G. Iaccarino, "Computation of turbulent Prandtl number for mixed convection around a heated cylinder," Center for Turbulence research, Annual Research Briefs 2010. pp. 295-304 (2010)

11. A.J. Reynolds, The prediction of turbulent Prandtl and Schmidt numbers, *Int. J. Heat and Mass Transfer* **18,** pp. 1055-1069 (1975).

12. W.M. Kays, Turbulent Prandtl number-Where are we, *Journal of Heat Transfer* **116** (May) pp. 284-295 (1994).

13. J.A Schetz, *Boundary Layer Analysis*, Prentice Hall, Englewood Cliffs, New Jersey, p 273 (1993).

14. F.M. White, Viscous Fluid Flow, 2nd ed. McGraw Hill, Int. Ed., p. 482 (1991).

15. J.H. Bae, J.H. Yoo, H. Choi, "Direct numerical simulation of turbulent supercritical flows with heat transfer," *Physics of Fluids* **17,** 105104 (2005).

16. W. Kays, M. Crawford, B. Weigand, *Convective Heat and Mass Transfer*, 4th ed., McGraw Hill International Edition, p. 185 (2005).

17. A. Quarmby, R. Quirk, "measurements of the radial and tangential eddy diffusivities of heat and mass in turbulent flow in a plain tube," *Int. J. Heat Mass Transfer*, **15**, pp. 2309-2327 (1972).

18. J.A Schetz, *Boundary layer Analysis*, Prentice Hall, Englewood Cliffs, New Jersey, p. 340 (1993).

19. W. Kays, M. Crawford, B. Weigand, *Convective Heat and Mass Transfer*, 4th ed., McGraw Hill International Edition, p. 264 (2005).

20. W. Kays, M. Crawford, B. Weigand, *Convective Heat and Mass Transfer*, 4th ed., McGraw Hill International Edition, pp. 233-239 (2005).

21. Y. Y. Bae, "A new formulation of variable turbulent Prandtl number for heat transfer to supercritical fluids with strong property variation," *Int. J. Heat and Mass Transfer,* (submitted)

22. T. Cebici, *Analysis of Turbulent Boundary Layers*, Academic Press, New York, San Francisco, London (1974).

23. J.D. Jackson, "Ideas for an Improved Semi-Empirical model of Turbulent Mixed Convection Hat Transfer to Fluids at Supercritical pressure," *The Proceedings of the 15th International Topical Meeting on Nuclear Reactor Thermal - Hydraulics, NURETH-15*, NURETH15-373, Pisa, Italy, May 12-17 (2013).

24. H.K. Myong, N. Kasagi, A new approach to the improvement of k–ε turbulence model for wall bounded shear flows, *JSME International Journal* **33**, pp. 63–72 (1990).

25. J. H. Ferziger, M. Peric, *Computational Methods for Fluid Dynamics*, Springer-Verlag, Berlin Heidelberg, (1999).

26. P. G. Huang, G. N. Coleman, P. Bradshaw, "Compressible turbulent channel flows: DNS results and modelling," Journal of Fluid Mechanics **305,** pp. 185-218 (1995).

27. H. Foysi, S. Sarkar, R. Friedrich, Compressibility effects and turbulence scalings in supersonic channel flow, *Journal of Fluid Mechanics* **509**, pp. 207-216 (2004).

28. M. Zhao, H. Gu, X. Cheng, Experimental study on heat transfer to supercritical water flowing through tubes, *Proceedings of ICAPP'12*, Paper 12368 (2012).

29. G.V. Alekseev, V.A. Silin, A.M. Smirnov, V.I. Subbotin, "Study of the thermal conditions on the wall of a pipe during the removal of heat by water at a supercritical pressure," Translated version of *Teplofizika Vysokith Temperatur* **14**(4), pp. 769-774 (1976).